Available online at www.sciencedirect.com
SCIENCE DIRECT
Polymer 46 (2005) 10688–10698
polymer
www.elsevier.com/locate/polymer

Nanofibers of self-doped polyaniline

Chien-Hsin Yang[a,*], Yi-Kai Chih[a], Hsyi-En Cheng[b], Cheng-Ho Chen[a]

[a] *Department of Chemical and Material Engineering, Southern Taiwan University of Technology, Tainan 710, Taiwan, ROC*
[b] *Department of Electric Engineering, Southern Taiwan University of Technology, Tainan 710, Taiwan, ROC*

Received 7 July 2005; received in revised form 9 September 2005; accepted 13 September 2005
Available online 29 September 2005

Abstract

Self-doping polyaniline (SPANI) nanofibers were synthesized by using self-assembly process consisting of a self-doping monomer (*o*-aminobenzenesulfonic acid, SAN) and aniline (AN). SAN plays the key roles of a self-doping monomer and a surfactant in the process of forming nanofibers. TEM and SEM results revealed that the morphology, average diameter of the resulting nanofibers depended on the mole ratio of AN to SAN and reaction conditions. NMR, FTIR, XPS, UV–vis spectra were used to describe the molecular structures of the nanofibers. X-ray diffraction was used to characterize the crystallinity in these structures. Results revealed that the molecular structures of polymer chains were similar to those of the emeraldine form of polyaniline (PANI). The doping degree ranged from 21 to 27% corresponding to the AN/SAN mole ratio from 4 to 1.

Keywords: Self-doping polyaniline (SPANI); Nanofibers; Self assembly

1. Introduction

Nanostructural materials have attracted much attention since the discovery of carbon nanotubes [1]. These materials have diverse potential applications such as nanoelectronics and biomedical devices [2]. Owing to long conjugated length and metal-like conductivity [3,4], conducting polymers are considered to a potential material in this area of applications. Nanostructures of conducting polymers have been synthesized by a template method, these polymers included polyacetylene [5], polypyrrole [6], poly(3-methylthiophene) [7] and polyaniline [8]. In our laboratory, the nanofibers of SPANI were produced by self-assembly process in the presence of SAN as a self-doping monomer. Here, SAN acted as a template in the formation of PANI nanofibers due to its functional group ($-SO_3H$).

However, the method in this study is very different from the methods of template and an external addition of dopant [9,10]. Unlike the two methods, SAN did not need to be removed after polymerization because it acted as a dopant and was linked in the polymer chains at the same time. In fact, this belongs to a self-assembly process. SAN monomer used in this experiment has both functions of a dopant and a surfactant. The function of surfactant demonstrated a key role in the formation of nanostructures of conducting polymers [11]. Therefore, it is interesting to clarify the surfactant function of this active SAN monomer through the examination of nanofiber formation using a self-assembly process.

In this work, SPANI nanofibers with an average diameter of 120–370 nm are reported for the first time. The effects of AN/SAN mole ratio and reaction conditions on the morphology, size, and some properties of these SPANI nanofibers were studied.

2. Experimental section

2.1. Materials

Aniline (Merck) was distilled under reduced pressure. *o*-Aminobenzenesulfonic acid (SAN, Aldrich) was recrystallized two times in distilled water. Oxidant (ammonium peroxydisulfate, APS, Aldrich) was used as received.

2.2. Synthesis of SPANI nanofibers

The nanofibers of SPANI were synthesized by a self-assembly method. AN and SAN ([AN]+[SAN]= 0.055 mol/L) were dissolved in 100 mL of distilled water, then an aqueous solution of APS (0.57 g in 12.5 mL of distilled water) was added to the above mixture under stirring for 2 min.

* Corresponding author. Tel.: +886 6 2533131x6959.
E-mail address: yangch@mail.stut.edu.tw (C.-H. Yang).

0032-3861/$ - see front matter © 2005 Elsevier Ltd. All rights reserved.
doi:10.1016/j.polymer.2005.09.044

The polymerization was carried out in a stationary condition at 4 °C. In order to perform the following analyses, a dark green solid of SPANI was collected on the surface of reaction solution and thoroughly rinsed using H_2O and CH_3OH, and then dried under vacuum for 24 h.

2.3. Scanning electron microscopy (SEM)

SEM micrographs of SPANI nanostructures were taken by a Philips XL-40 FEG scanning electron microscope.

2.4. Transmission electron microscopy (TEM)

The morphology was measured by a transmission electron microscope (TEM, JEM-1230, JEOL Ltd, Japan) with an acceleration voltage of 80 kV.

2.5. XPS measurements

The XPS measurements were performed with ESCA 210 and MICROLAB 310D (VG Scientific Ltd) spectrometers. XPS spectra was recorded with Mg K_α ($h\nu = 1253.6$ eV) irradiation as the photon source with a primary tension of 12 kV and an emission current of 20 mA. Analysis chamber pressure during the scans was kept approximately as 10^{-10} mbar.

2.6. Solid-state NMR analysis

Solid-state ^{13}C magic angle spinning (MAS) NMR experiments were performed on a Bruker AVANCE-400 spectrometer, equipped with a Bruker double-tuned 7 mm probe, with resonance frequencies of 100.6 MHz for ^{13}C nuclei at 298 K. The Hartmann–Hahn condition for $^1H \rightarrow {}^{13}C$ cross-polarization (CP) experiments was determined using admantane. The $\pi/2$ pulse lengths for ^1H and ^{13}C were typically 4 and 6 μs, respectively. A repetition time of 4 s was used. The ^{13}C chemical shifts were externally referenced to tetramethylsilane (TMS). The $^1H \rightarrow {}^{13}C$ CP spectra were recorded as a function of contact time using a single-contact pulse sequence with reversal of spin temperature in the rotating frame and with high-power proton decoupling during the ^{13}C signal acquisition.

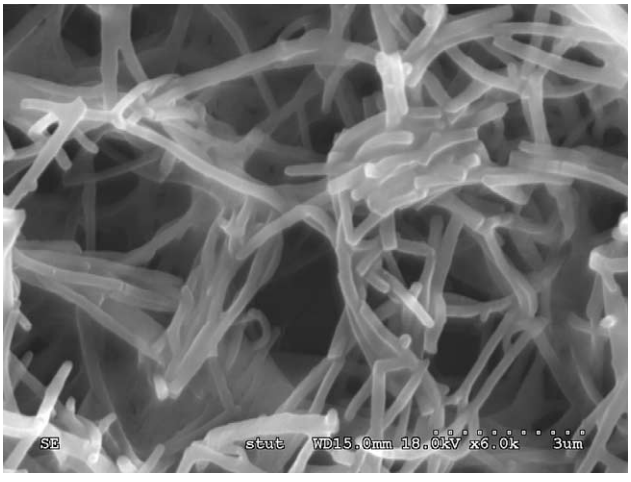

Fig. 1. SEM images of SPANI nanofibers with AN/SAN mole ratio of 1.

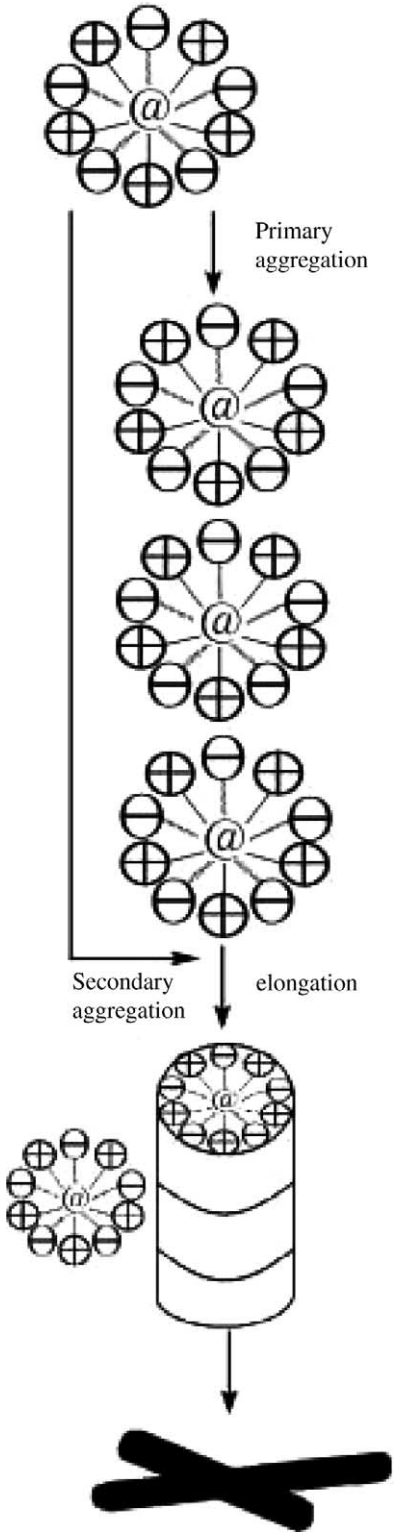

Scheme 1. Schematic presentation of the formation mechanism for SPANI nanofibers synthesized by a self-assembly process.

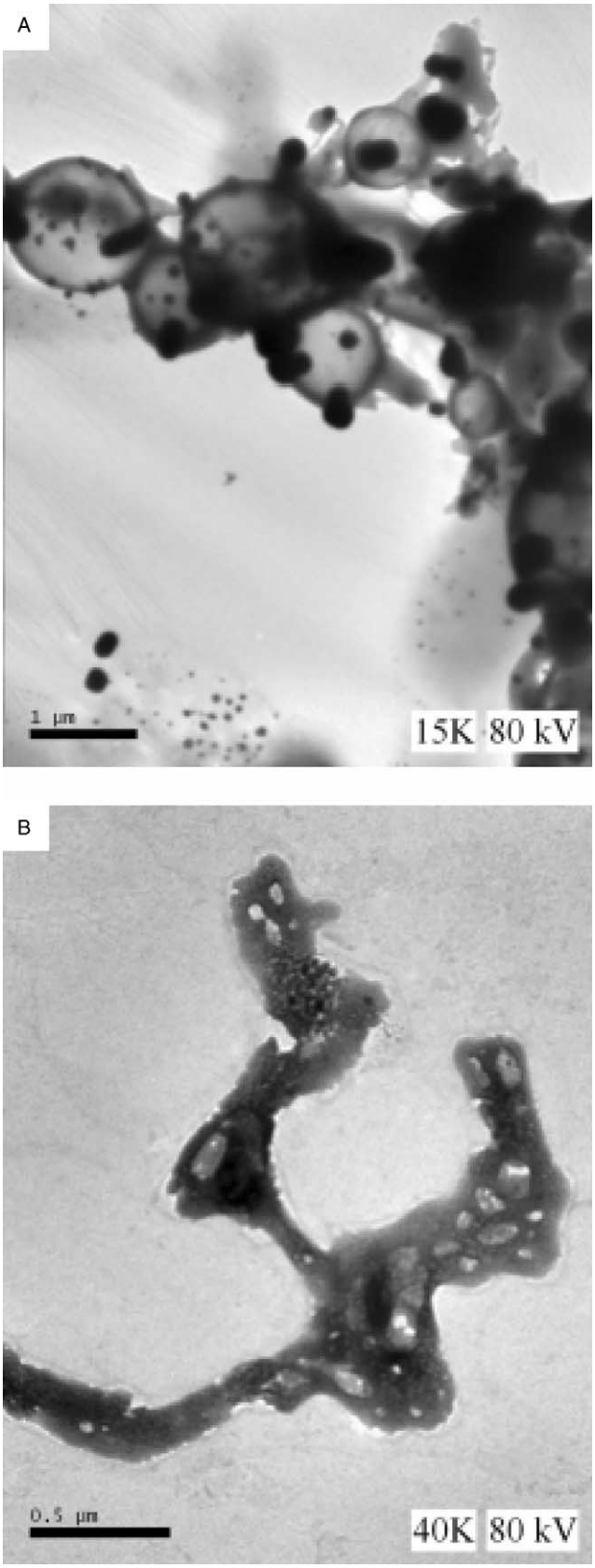

Fig. 2. TEM images of (A) a freeze-fracture replica sample with AN/SAN mole ratio of 1.0 after 1 h assembly time; (B) aggregated micellar AN-SAN (AN/SAN = 1.0) spheres coexisting with sub-micrometer-sized structure, which have the tendency to form fiber junctions after 5 h assembly time.

2.7. FT-IR analysis

The sample was prepared by mixing 1 wt% polymer with KBr to form a pellet. Infrared spectra were obtained with a Fourier transform IR spectrophotometer (Nicolet FTIR 550) and recorded by averaging 64 scans at a solution of 4 cm^{-1}.

2.8. UV–vis analysis

UV–vis absorption spectra were recorded on a Shimadzu diode-array spectrophotometer (UV-2401 PC).

2.9. XRD analysis

XRD patterns of SPANI nanofibers were obtained by using an X-ray diffractometer (Rigaku multiflex ZD3609N, Rigaku Co., Japan). Cu K_α ($\lambda = 0.154$ nm) radiation was adopted at room temperature. The scanning rate was kept at 2°/min in the range of 2–50°.

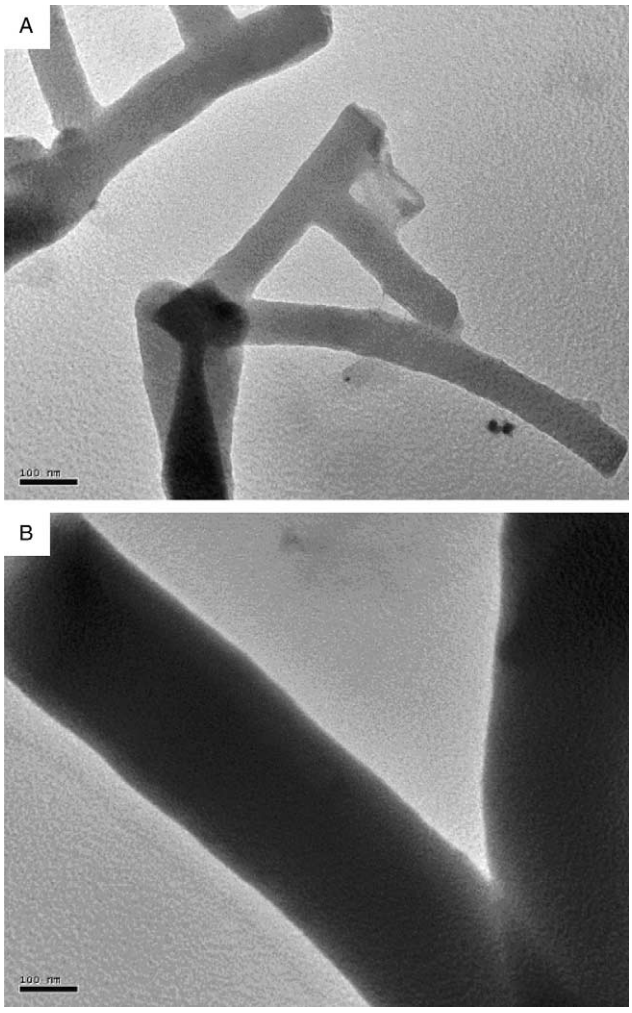

Fig. 3. TEM images of SPANI nanofibers with AN/SAN mole ratios: (A) 4.0 and (B) 1.0.

2.10. Conductivity

The conductivity at room temperature was measured by a Keithley 2400 with an ADVANTEST R6142 programmable Dc voltage/current source, a standard four-probe method.

3. Results and discussion

3.1. Morphologies of SPANI nanofibers

SEM images of SPANI samples are shown in Fig. 1, revealing dendrite morphology. SAN is used as a surfactant and a monomer (represented by $\Theta\sim\sim\sim$), which is easy to form micelles; whereas aniline may exist in the form of anilinium cations (represented by $\oplus$—) or aniline (represented by @) in the reaction solution. SAN and aniline cations first form micelles in aqueous solution. Anilinium cations can be solubilized in the micelle-water interface to form micelle, a part of AN diffuses in micelles as shown in Scheme 1. Micelles were regarded as the templates to further produce SPANI nanofibers. At the addition of the oxidant (APS), the polymerization initially performed on the surface of the micelles. Solubilized aniline or anilinium molecules are oxidatively polymerized by APS in the aqueous solution [12]. With the polymerization proceeding, because SPANI is a rigid molecule, the micelles thus tend to join along the direction of

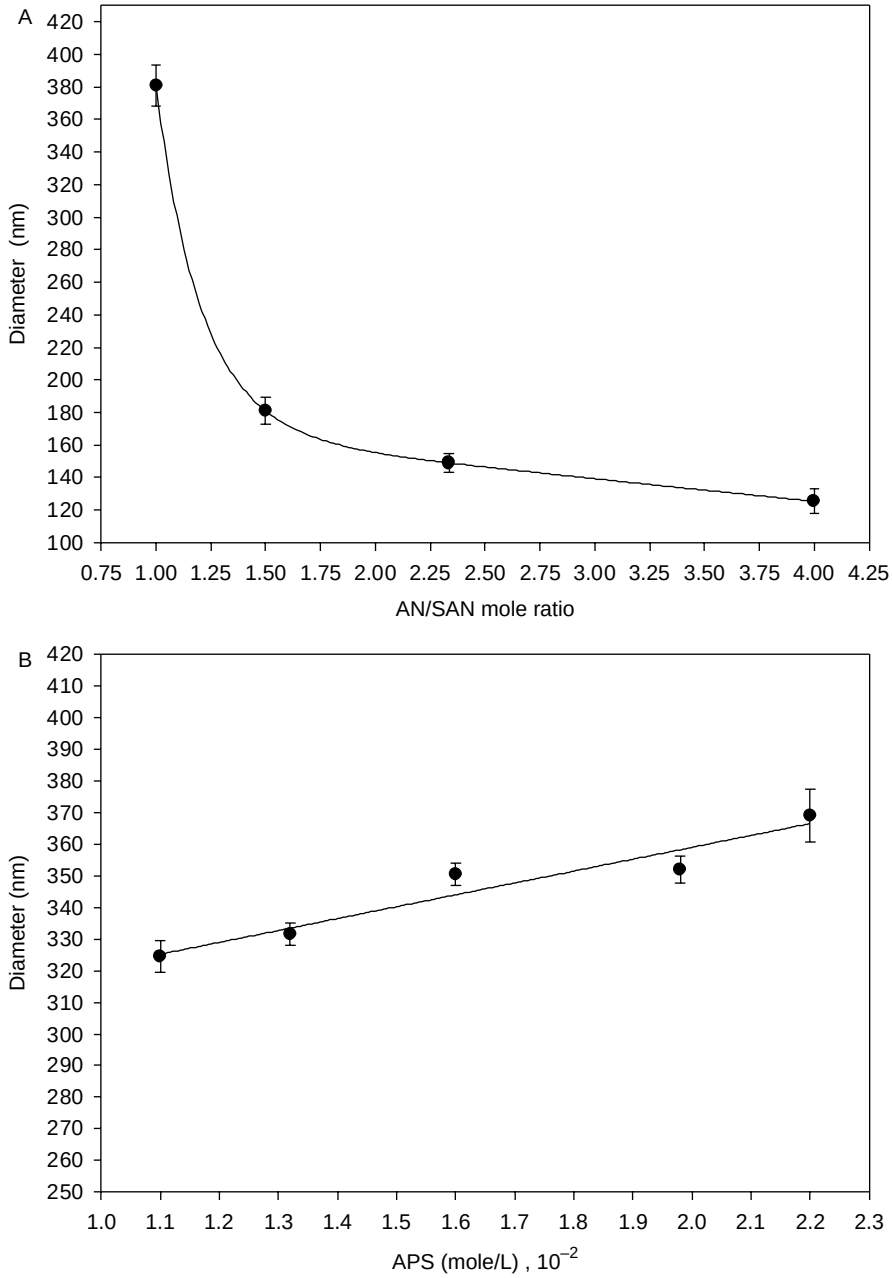

Fig. 4. Dependence of the average diameter of SPANI nanofibers on (A) AN/SAN mole ratio; (B) the concentration of APS; (C) total concentration of monomers ([AN]+[SAN]); (D) the reaction temperature, and (E) the self-assembly time. The results from (B) to (E) were performed with AN/SAN mole ratio of 1.

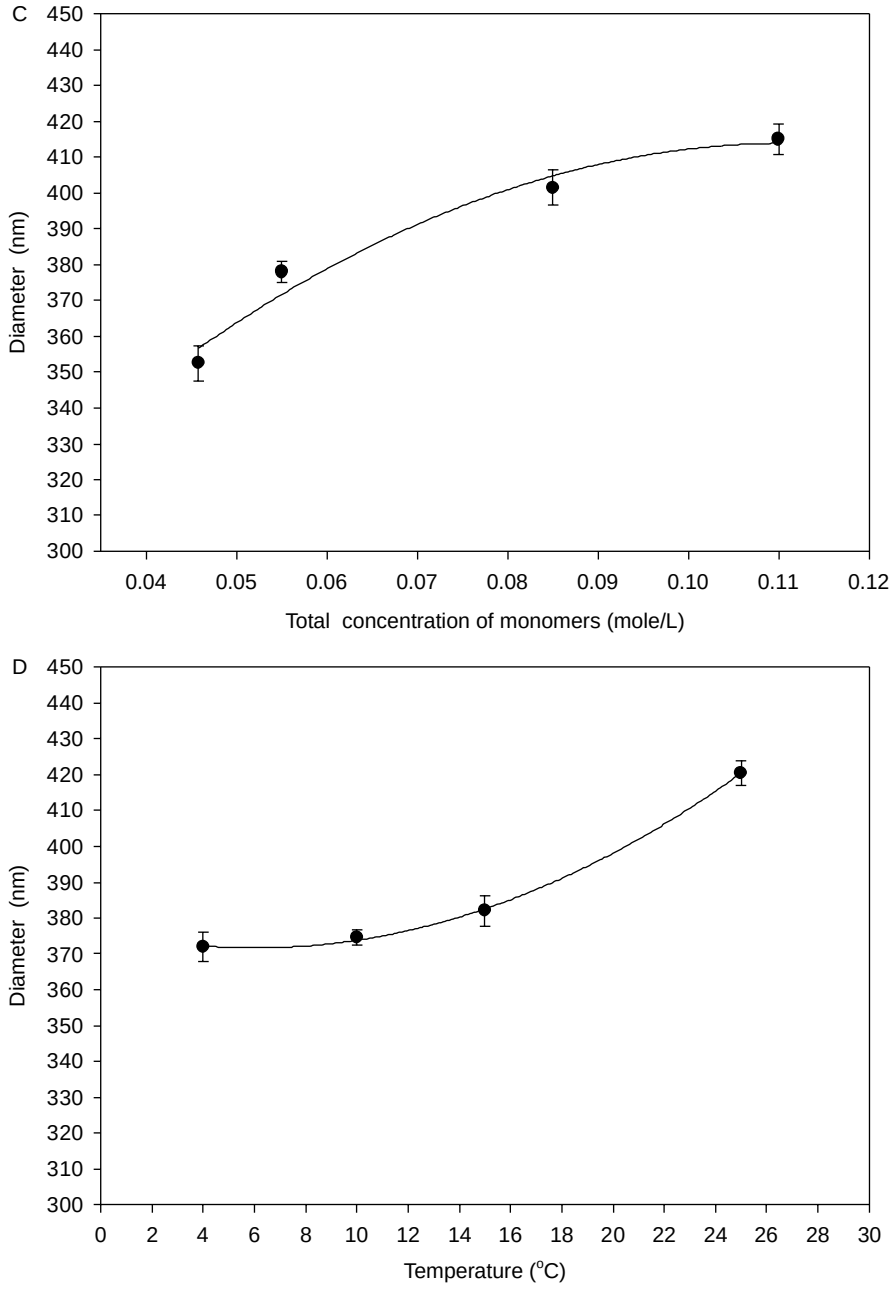

Fig. 4 (*continued*)

the polymer chain in the polymerization process. Therefore, the polymer chain acted like a template in the self-assembly of SPANI nanofibers. Fiber structures are assembled by the micelles through aggregation and elongation [13] depending on the local conditions. In our work, it is obvious that the morphology of the resulting SPANI nanofibers exhibits the existence of the elongation procedure. In this Scheme, micelles will be converted into fibers. Because the reaction proceeded in a stationary environment, the primary aggregation of micelles may mainly affect the size of the resulting nanostructures; on the other hand, the secondary aggregation of other micelles near the formed nanofibers will yield branched structures, which served as templates for nanostructural junctions and dendrites. Actually, spherical micelles existed in the reaction system (Fig. 2(A)), whereas the micelle spheres aggregated to form a branched structure coupled with the sumicrometer-sized fibers in the resulting SPANI (Fig. 2(B). These results reflect that the micelles cannot only fuse to form sub-micrometer-sized fibers, but can also aggregate to form sub-micrometer-sized fiber junctions and dendrites through a self-assembly process. Moreover, these micelles will fuse and shrink to form nanofibers in this self-assembly process. The statement of Scheme 1 can be strongly supported by TEM images of the freeze-fracture replica samples (Fig. 2).

From an examination of TEM images (Fig. 3), SPANI showed a loose nanofibril structure corresponding to AN/SAN

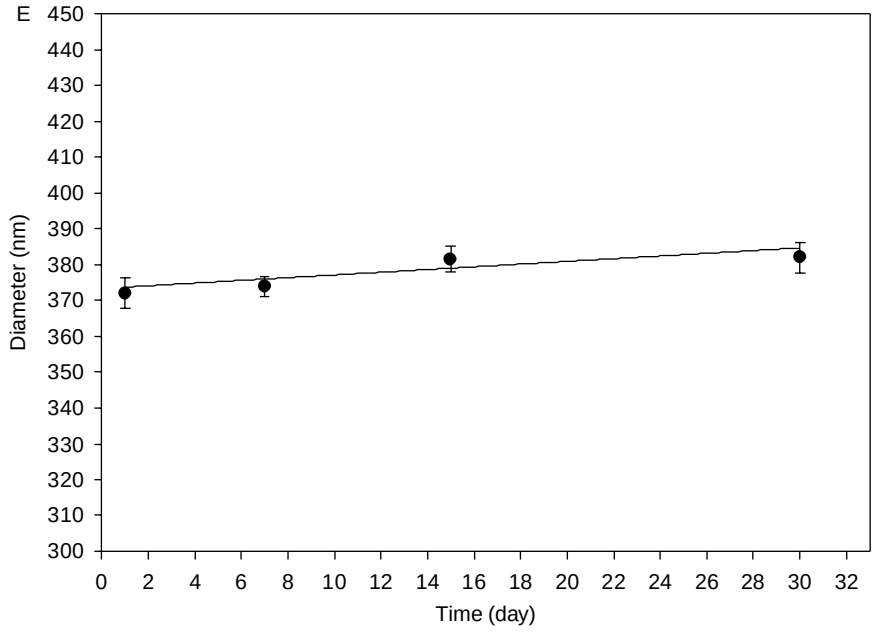

Fig. 4 (*continued*)

mole ratio of 4 (Fig. 3(A)); whereas SPANI exhibited a dense nanofibril structure corresponding to AN/SAN mole ratio of 1 (Fig. 3(B)). One possible explanation for this result is that the two kind of aggregation may be affected by the interactions among polymer chains, for example, π–π interactions, hydrogen bonding, and ionic bonding [14]. In our work, the average diameter of SPANI samples varies with the different composition of AN/SAN mole ratio. Actually, it was found that the size of the nanofibers strongly depended on the mole ratio of AN/SAN and reaction conditions (e.g. reaction temperature, APS concentration and total concentration of monomer). In Fig. 4(A), the diameter of SPANI nanofibers decreases with increasing AN/SAN ratio. In micelles, the sulfonate content (SAN) of low AN/SAN ratio is higher than that of high AN/SAN ratio, existing a stronger interactions among polymer chains as follows.

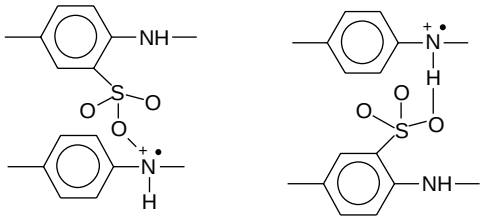

The aggregation of micelles is significantly enhanced by these interactions. This leads to a larger diameter of nanofibers in the self-assembly process. Meanwhile, this kind of interactions between polymer chains further supports the existence of a dense nanofiber structure at high SAN content. These results also suggest that the diameter of SPANI nanofibers is controllable by adjusting the AN/SAN mole ratio. Moreover, the size of SPANI nanofibers was affected by the concentration of APS. Taking AN/SAN mole ratio of 1 as an example (Fig. 4(B)), the diameter of this system increased from 320 to 370 nm when APS concentration changed from 1.0 to 2.0 mol/L. One possible explanation for this result is that the interactions among polymer chains increase with the increase of APS content involving SPANI matrix. Also, the size of SPANI nanofibers greatly depends on the total concentration of monomers ([AN] + [SAN]) as shown in Fig. 4(C). It is obvious that the diameter increases with increasing the total concentration of monomers. This result is attributable that the aggregation of micelles is more significant at higher total concentration of monomer in the self-assembly process, leading to a larger diameter of nanofibers. The converse is true. In addition, the size of SPANI nanofibers was slightly changed with the variation of reaction temperature. In Fig. 4(D), the diameter of these nanofibers increased from 370 to 425 nm corresponding to the temperature variation from 4 to 25 °C. This implies that the aggregation of micelles is enhanced with the increase of temperature, resulting in larger diameter of these nanofibers. It is noteworthy that the diameter of these nanofibers almost keeps constant with the increase of incubation time (Fig. 4(E)). This result further supports that the size of SPANI nanofibers is dominated by the primary aggregation within 24 h. After this period, the effect of the primary aggregation is insignificant with the self-assembly time.

3.2. Chemical analysis

Wide scanning provides a determination of which elements were present in an SPANI sample. A typical XPS survey scan of the SPANI (with AN/SAN ratio of 1) reveals that C, N, O, and S signals are detected in this polymer sample. The relative concentrations of C, N, O, and S in the polymer, calculated from the corresponding photoelectron peak area after sensitivity factor corrections (SF = 1.00, 1.77, 2.14, and 2.85 for C_{1s},

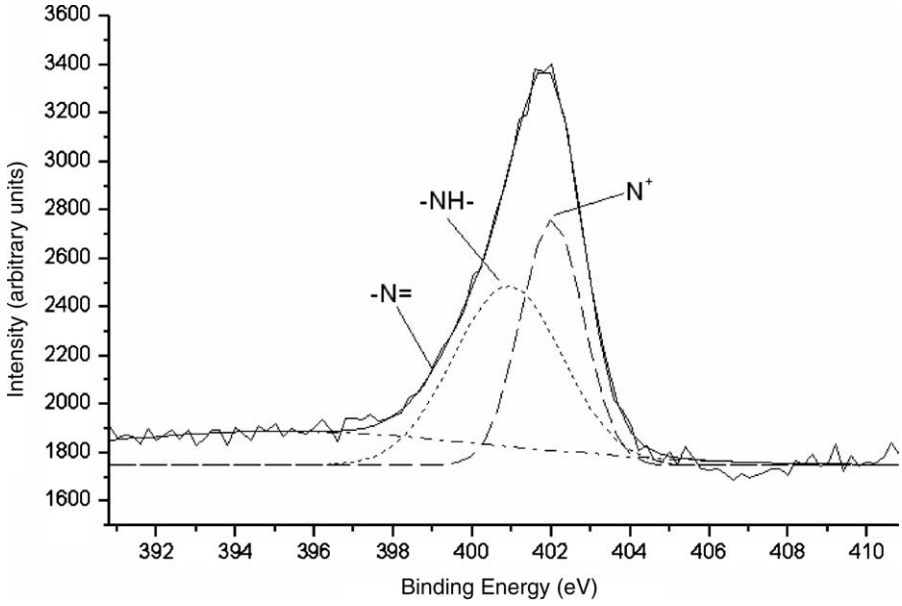

Fig. 5. N_{1s} XPS core-level spectra of the SPANI with AN/SAN mole ratio of 1.

N_{1s}, S_{2p}, and O_{1s}, respectively). The N_{1s} core-level spectra of the SPANI nanofibers have been deconvoluted by assigning binding energies of 399.1, 400.1, and 402.0 eV for the imine (–N=), amine (–NH–), and polaron specis (N^+), respectively [15], as illustrated by the spectra in Fig. 5. Note that the second component peak (amine site) is dominant in the N_{1s} core-level spectrum of these SPANIs. The formation of N^+ (polaron site) is due to the nitrogen in the vicinity of H^+ cations when the polymers were self-doped with $–SO_3H$ groups (bearing on the polymer chain). On the other hand, the imine site arises from the strong hydrogen bonding of –NH to oxygen atoms. The doping degree, defined as $[N^+]/[N]$, is shown in Fig. 6 revealing that the doping degree increases with increasing SAN concentration. It is reasonable that the concentration of H^+ cations increases with increasing $–SO_3H$ content, and this increase results in a higher probability of nitrogen attaching to the H^+ cations. This explanation is consistent with the content of sulfur on the polymer chain (Fig. 6). Furthermore, the S/N ratio is lower than the feed ratio of SAN in the comonomers, indicating that the polymerization rate of AN is faster than that of SAN. Also note that the doping degree ($[N^+]/[N]$ (%)) is smaller than the value of S/N ratio. This reflects that the $–SO_3H$ groups are not completely used to dope the nitrogen atoms on the polymer chain.

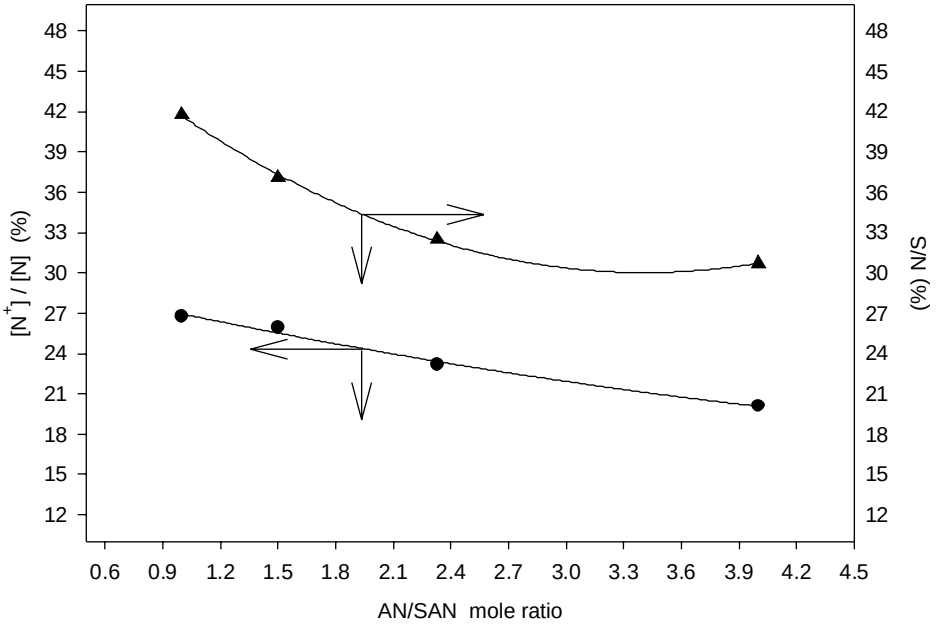

Fig. 6. Effects of AN/SAN mole ratio on the doping degree (N^+/N (%)) and S/N value of SPANI nanofibers.

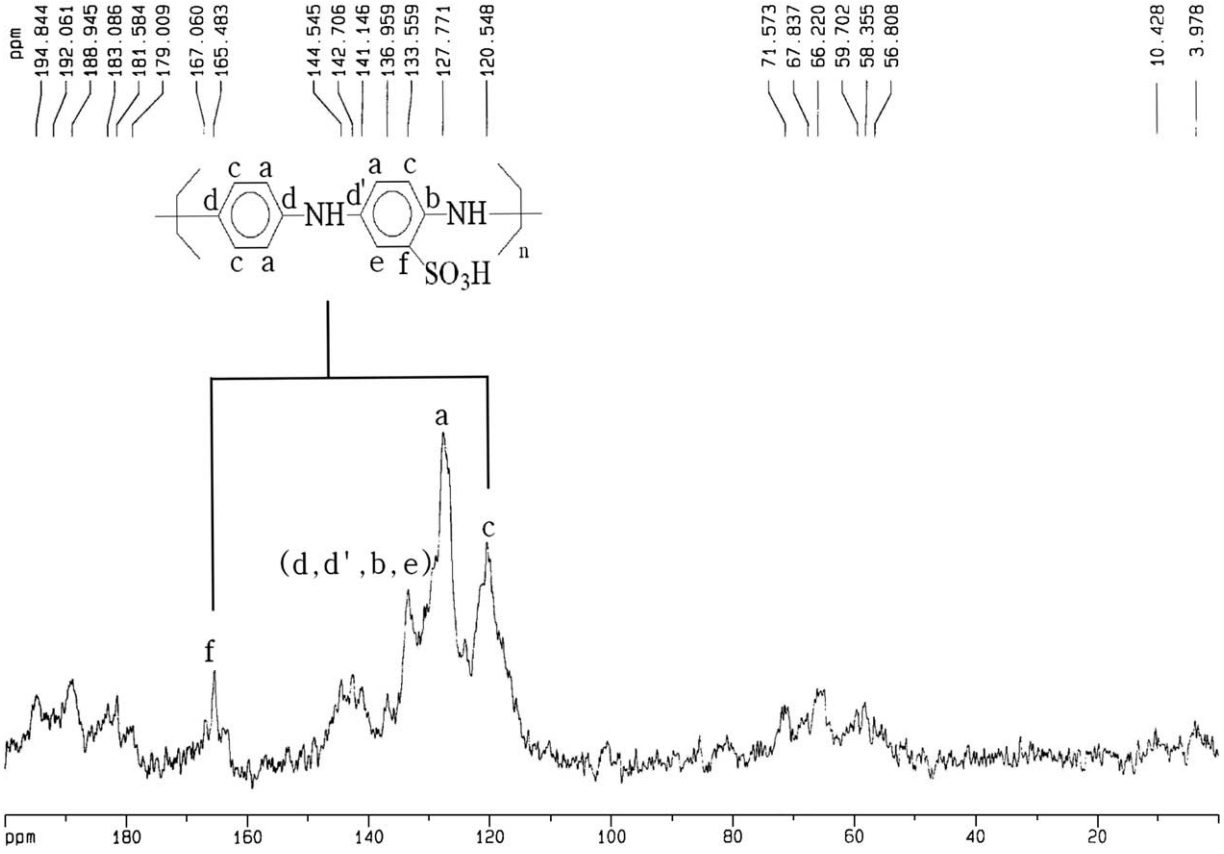

Fig. 7. Aromatic region of the ^{13}C NMR spectrum of SPANI with AN/SAN mole ratio of 1 at 298 K.

3.3. Structural characterization

NMR, FT-IR, UV–vis spectra, and X-ray diffraction were used to characterize the molecular structure of the resulting nanofibers of SPANI with different AN/SAN mole ratio.

NMR analyses indicate clearly that well-defined SPANIs have been indeed obtained. As an example with its simple repeat unit, we show here the ^{13}C NMR spectra (Fig. 7) of these SPANIs. The aromatic region of the ^{13}C NMR spectrum of SPANI supports the regiochemical structure of the polymer. In

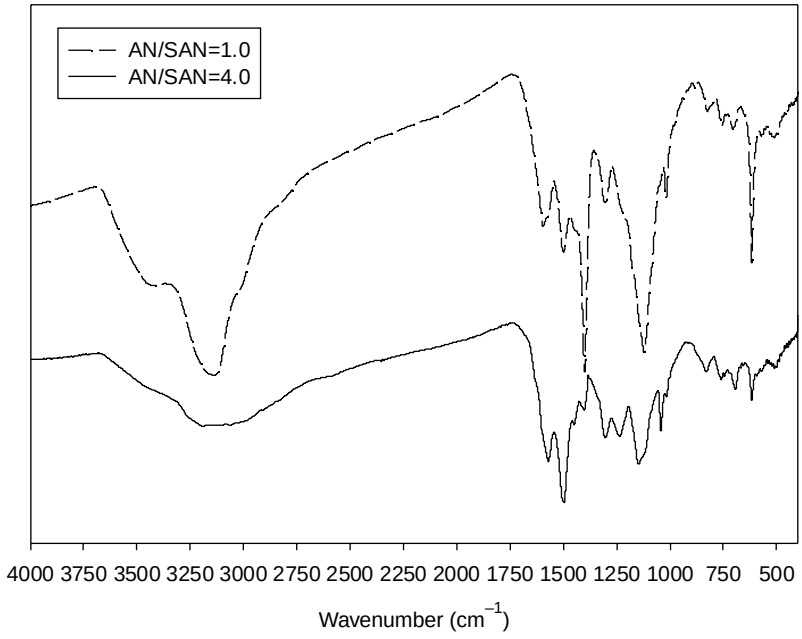

Fig. 8. FT-IR spectra of SPANI nanofibers with different AN/SAN mole ratios.

this figure, only five obvious peaks appear in the aromatic region, which are related to the 12 aromatic carbon atoms of the partial symmetric repeating units (AN and SAN). In addition, this ^{13}C NMR spectrum shows some additional small peaks, suggesting that the distortion on polymer chains occurs in these SPANI nanofibers. This information confirms that the polymer nanofibers prepared from a self-assembly process are region-irregular.

Fig. 8 shows the FT-IR spectra of SPANI nanofibers prepared with two different AN/SAN mole ratio of 4 and 1, respectively. It was found that the FT-IR spectra of the two samples were similar. The characteristic peaks around 1567 and 1483 cm^{-1} are assigned to the stretching vibration of quinoid ring and benzenoid ring, respectively. The bands at 1300 and 1246 cm^{-1} correspond to C–H stretching vibration with aromatic conjugation. Actually, these peaks are similar to those of PANI-(β-NSA) microtubes[12] and those of PANI-HCl prepared in a common method. These results suggest that the backbone structures of these SPANI nanofibers obtained in this study are similar to each other and also to those of PANI-(β-NSA) microtubes [16] and those of PANI-HCl [17] reported elsewhere.

UV–vis spectra of the resulting SPANI nanofibers dissolved in *m*-cresol were measured and shown in Fig. 9. The band at $\lambda^{I}_{max} = 307$ nm (band I) corresponds to the reduced state (leucoemeraldine) of PANI. The band II (at $\lambda^{II}_{max} = 421$ nm)

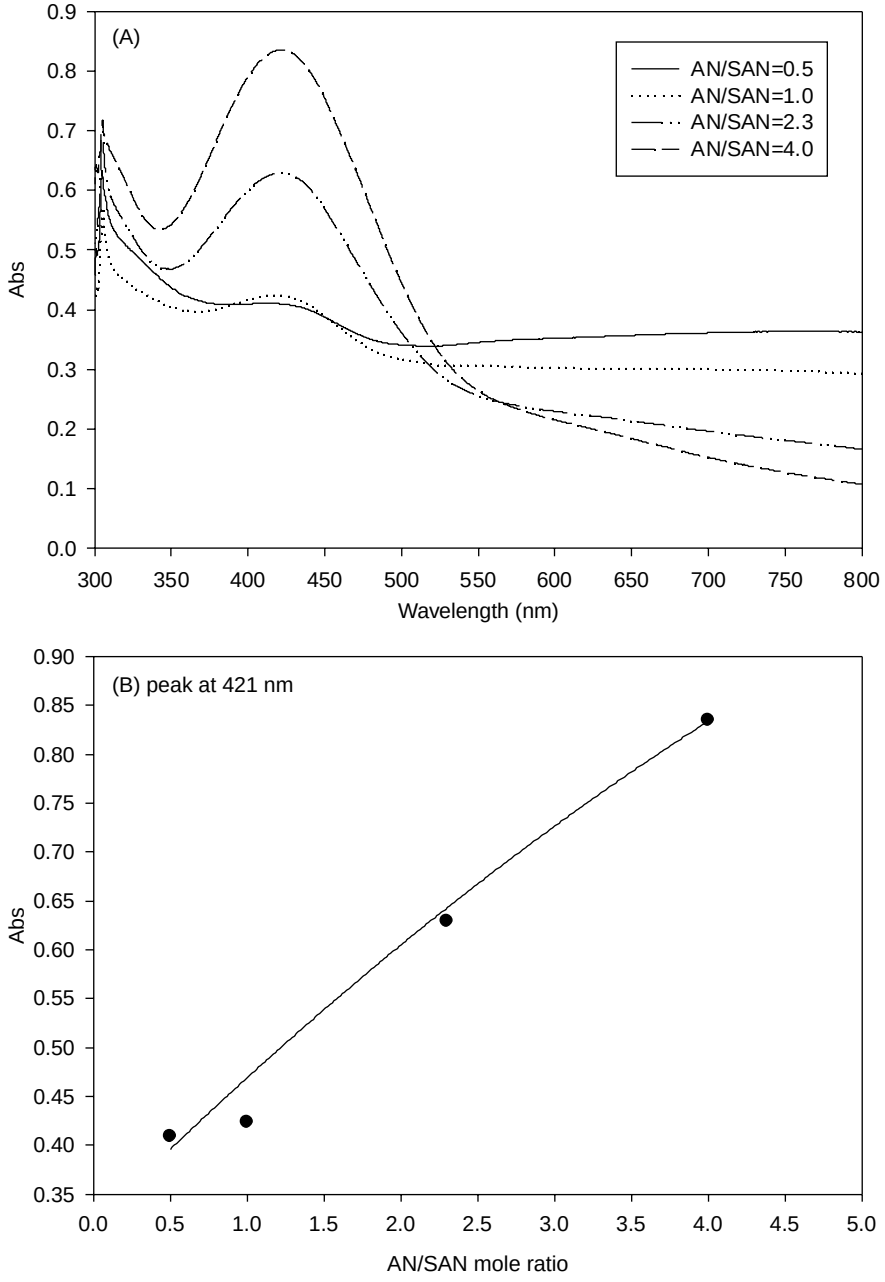

Fig. 9. (A) UV–vis spectra of the resulting SPANI nanofibers dissolved in *m*-cresol. (B) Influence of AN/SAN mole ratio on the absorbance of band II corresponding to $\lambda^{II}_{max} = 421$ nm.

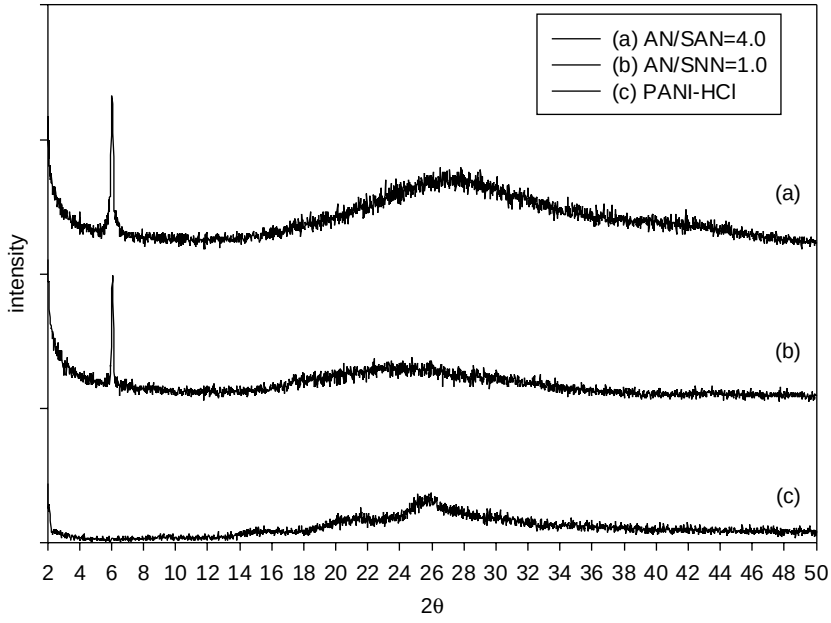

Fig. 10. X-ray scattering patterns of SPANI nanofibers with different AN/SAN mole ratios and PANI doped with HCl.

corresponds to partial oxidation of PANI and can be assigned to represent the intermediate state between leucoemeraldine form containing benzenoid rings and emeraldine form containing conjugated quinoid rings in the main chain of the PANI. The emeraldine form transforms into fully oxidized pernigraniline form and characterized by a wide band at around 800 nm. An increase in intensity for the band II was noted (Fig. 9(B)) when the AN/SAN ratio was increased to higher value. This implies that the intermediate state between the transition of leucoemeraldine to emeraldine form increases with the increase of AN/SAN ratio. This result reflects that this transition would be inhibited by the addition of SAN. On the other hand, the intensity of band III decreases with increasing AN/SAN ratio. This indicates that the degree of self-doping decreases with increasing AN/SAN ratio, leading to a decrease of polaron band (band III) [18]. However, these SPANI nanostructures are presented as the emeraldine salt form of PANI [19].

X-ray diffraction patterns of SPANI and PANI are shown in Fig. 10. A broad peak centered at $2\theta = 27°$ was observed with the AN/SAN ratio of 4, but a different broad peak around $2\theta = 22°$ was present with the AN/SAN ratio of 1. The peak centered at $2\theta = 22°$ could be caused by the periodicity parallel to the polymer chain, whereas the peak around $2\theta = 27°$ is attributed to the periodicity perpendicular to the direction of polymer chain [20]. It is worth noticed that the crystallinity of SPANI nanofibers in this work is similar to that of PANI-doped external dopants [10]. These two resulting nanofibers show amorphous. In particular, the unusual sharp peak around $2\theta = 6°$ assigned to the scattering along the orientation parallel to the SPANI chain [16], which corresponds to a crystallographic spacing (d). It is clear that this peak in these polymer nanofibers is obvious. This sharp peak is absent from PANI-external dopant (HCl) synthesized by a common method. Bragg's law, $n\lambda = 2d\sin\theta$, was used to calculate the crystallographic spacing (d). The basal spacing of 1.47 nm was obtained corresponding to the nanofibers with AN/SAN ratio of 4. And, the value of 1.45 nm was obtained corresponding to the nanofibers with AN/SAN ratio of 1. These data reflect that these nanofibers are formed by a layer-assembly which is very different with PANI powder.

3.4. Conductivity

The effect of AN/SAN mole ratio on the conductivity of SPANI was measured and shown in Fig. 11. There was significant difference in conductivity with the range of 10^{-5}–10^{-6} S cm^{-1}, when AN/SAN varied from 0.25 to 4.0. This result is almost consistent with the doping degree as shown in Fig. 6. The conductivity decreases with increasing the AN/SAN ratio due to a decrease in doping degree at AN/SAN > 1.0. It is noteworthy that the maximum conductivity exists at AN/SAN ratio of 1.0. The conductivity inversely decreased as SAN increased to above 1.0 of AN/SAN ratio in the monomer

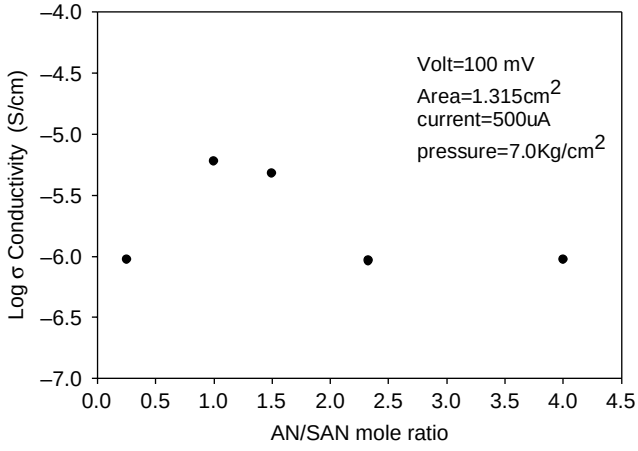

Fig. 11. Effect of AN/SAN on room temperature conductivity of SPANI pellets.

mixture. This result may be attributed to the formation of lower molecular weight polymer at relatively high SAN content in the comonomer.

4. Conclusions

Nanofibers of SPANIs, with a diameter of 120–370 nm, were successfully synthesized by a self-assembly process. It was found that the average diameters of these SPANI nanofibers could be controlled through adjusting AN/SAN mole ratio in the monomers. In particular, SAN played the key roles of an active monomer and a surfactant. In the presence of SAN, micelles formed by anilinium cations and surfactant anions of SAN were regarded as templates in the formation of the nanofibers. XPS results proved that SAN molecules had been incorporated in polymer chains and the doping degree possessed 21–27% depending on the AN/SAN mole ratio. Moreover, the resulting nanofibers are amorphous. This innovative self-assembly method may open a new route to synthesize functional nanofibers of conducting polymers.

Acknowledgements

This study was supported by the project of the National Scientific Council of the Republic of China (NSC-93-2622-E-218-021-CC3 and NSC-94-2214-E-218-003) is greatly appreciated.

References

[1] Iijima S. Nature (London) 1991;354:56.
[2] Lei J, Menon VP, Martin CR. Polym Adv Technol 1992;4:124.
[3] Cao Y, Smith P, Heeger AJ. Synth Met 1992;48:91.
[4] Martin CR. Science 1994;266:1961.
[5] Liang W, Martin CR. J Am Chem Soc 1990;112:8976.
[6] Cai Z, Martin CR. J Am Chem Soc 1989;111:4138.
[7] Martin CR. Adv Mater 1991;3:457.
[8] Cai Z, Lei J, Liang W, Menon V, Martin CR. Chem Mater 1990;3:960.
[9] Zhang Z, Wei Z, Wan M. Macromolecules 2002;35:5937.
[10] Wei Z, Zhang L, Yu M, Yang Y, Wan M. Adv Mater 2003;15:1382.
[11] Wan MX, Li JC. J Polym Sci, Part A: Polym Chem 2000;38:2359.
[12] Kim BJ, Oh SG, Han MG, In SS. Synth Met 2001;122:297.
[13] Harada M, Adachi M. Adv Mater 2000;12:839.
[14] Kosonen H, Ruokolainen J, Knaapila M, Torkkeli M, Jokela K, Serimaa R, et al. Macromolecules 2000;33:8671.
[15] Yue J, Epstein AJ. Macromolecules 1991;24:4441.
[16] Huang J, Wan MX. J Polym Sci, Part A: Polym Chem 1999;37:151.
[17] MacDiarmid AG, Chiang JC, Halpern M, Huang WS. Mol Cryst Liq Cryst 1985;121:173.
[18] MacDiarmid AG, Epstein AJ. Synth Met 1994;65:103.
[19] Cao Y, Smith P, Heeger AJ. Synth Met 1989;32:236.
[20] Moon YB, Cao Y, Smith P, Heeger AJ. Polym Commun 1989;30:196.